Loss Analysis of Magnetic Gear with Slotted in Magnetic Modulation Ring

Can Tan, Wei Liu, Yingying Rao, Weizhao Tang, and Libing Jing

***Abstract*—In order to improve the operation efficiency of coaxial magnetic gear (CMG), in this paper, a CMG model with slotted in magnetic modulation ring is proposed. In this model, the permanent magnets (PMs) of internal and external rotors are distributed in Halbach array, the inner rotor PMs are equally divided into 3 small pieces, and the outer rotor PMs are equally divided into 2 small pieces. At the same time, the static magnetic modulation ring iron blocks are slotted, each iron block has 3 slots, the width of the slot is 0.4°, and the depth of the single side slot is 1mm. Finally, a two-dimensional model is established, and the eddy current loss and iron loss of the model are optimized, compared with the conventional CMG model, it is found that the changed pattern can increase the internal and external output torque by 4% and 4.12%, respectively. The eddy current loss is reduced by 66.57%, and the iron loss is reduced by 8.9%, which significantly improve the operation efficiency of the CMG.**

***Index Terms*—Coaxial magnetic gear, Electromagnetic torque, Halbach array, Loss, Slotting.**

I. Introduction

With the improvement of people's awareness of environmental protection, people gradually change from fossil energy to new energy. As a representative of new energy development, new energy vehicles and charging piles and so on have attracted extensive attention of researchers. During the process of rotation and torque transmission, the mechanical gear will be affected by its inherent problems. For example, under the condition of overload, the whole gear will be damaged due to different degrees of damage to the teeth of the mechanical gear. During normal operation, the meshing between the gears will produce noise and vibration, so it is necessary to maintain the mechanical gear regularly [1]-[4], which limits the scope of use of the mechanical gear. Compared with mechanical gears, magnetic gears have the advantages of high reliability, overload protection, physical isolation between input and output, maintenance free [5], [6]. Based on the defects of mechanical gears, magnetic gears have been effectively made up, so that magnetic gears have a broader application space and have been proposed by many scholars in the fields of wind, traction, and wave energy [7].

Early magnetic gears were similar in structure to mechanical gears, only including inner rotor and outer rotor. Due to its single topology, and the permanent magnet (PMs) can not be used to the maximum extent and the output torque density is lower than that of mechanical gear. Therefore, the early magnetic gear structure did not attract much attention of researchers [8]. K.Atallah and D.Howe optimized and improved the model structure of the gear, in 2001, they proposed a coaxial magnetic gear (CMG) based on the principle of magnetic field modulation. The pole pairs of the PMs of the internal and external rotator of the CMG are 4 pairs of poles and 22 pairs of poles, respectively. In addition, it also includes a magnetic regulating ring with 26 pairs of poles, the torque density of the prototype is measured to be 100KN·m/m^3 [9]-[11]. At any time, the internal and external rotator PMs of the structure can participate in the transmission of torque. Compared with the early magnetic gear structure, the concentric magnetic gear structure improves the utilization of permanent magnets. Based on the principle of CMG model structure, more structural models, such as harmonic, planetary and other model structures, have been proposed [12]. These magnetic gears can be applied to transmission systems with different requirements [13]. With the deepening of the research field of magnetic materials, a new permanent magnet material NdFeB appears in people's vision. Compared with other permanent magnet materials, NdFeB has better magnetic properties. The permanent magnet of magnetic gear is usually made of NdFeB, and its magnetization methods include radial magnetization, parallel magnetization and Halbach array magnetization. Different magnetization directions of PMs have diverse effects on the property of the equipment. Compared with the conventional radial magnetization and parallel magnetization, Halbach magnetization has many merits and applications [14]. In order to obtain higher torque density of magnetic gear, scholars have used magnetization mode with better performance, improved the shape of magnetic modulation ring and optimized various parameters of magnetic gear [15]. In [16], the CMG adopts Halbach magnetization mode, and the magnetic field and torque stability produced by this magnetization method are analyzed by simulation. The magnetic adjusting ring can modulate the magnetic field generated by the PMs, and its different shapes have different effects. Reference [17] compares the effects of different shapes of magnetic adjusting rings on the output torque characteristics

Manuscript received April 01, 2022; revised June 18, 2022; accepted July 21 2022. Date of publication March 25, 2023; Date of current version January 11, 2023.

This work was supported in part by National Natural Science Foundation of China and China Postdoctoral Science Foundation. (Project No. 51707072, 2018M632855). *(Corresponding author: Libing Jing.)*

C. Tan, W. Liu, Y. Rao, W. Tang and L. Jing are with the College of Electrical Engineering and New Energy, China Three Gorges University, Yichang, 443002, China (e-mail: jinglibing163@163.com).

Digital Object Identifier 10.30941/CESTEMS.2023.00001

of CMG. In [18], the CMG contains two magnetic modulation rings. In addition to the main magnetic modulation ring between the internal rotor and the external rotor, there is an auxiliary modulation ring outside the external rotor. The auxiliary adjusting ring can reduce the flux leakage outside the outer rotor, adjust it to useful harmonics and amplify its amplitude, so as to improve the torque transmitting ability of the CMG and the utilization rate of the PMs. In the conventional magnetic gear model, any one of the internal rotor, the external rotor and the magnet ring is set to a stationary state, and the other two parts rotate at a certain speed, so as to realize the power transmission of the fixed transmission ratio. Reference [19] proposed a torque transmission model that can realize the variable transmission ratio, which controls any one of the inner rotor, the outer rotor and the flux adjusting ring, so that it has a broader application field. Different permanent magnet materials have different properties. When installed in the equipment, the quality and volume of the equipment will be very different [20], [21]. In addition to optimizing the magnetic gear body, researchers also combine the magnetic gear with the motor, replace the internal rotor of the magnetic gear with the stator winding, and then form a magnetic gear permanent magnet composite motor. This composite structure can improve the torque and reduce the weight and size.

In [22], soft iron is used as the material of equipment, which is simple to manufacture, but the results show that its loss is large. Reference [23] analyzes the variation law of magnetic field of magnetic gear, and obtains the relationship between iron loss and speed. Reference [24] conducted a prototype test on the magnetic gear, and the connection curves between eddy current loss, iron loss and speed were obtained. At present, there are few literatures on the loss of magnetic gears. Most of them simulate it by software and then calculate the loss value. Although the above structure has higher torque density and better output torque, the problem of loss optimization is not discussed. Therefore, in order to obtain better torque and lower loss, it is necessary to study the magnetic gear.

In this paper, a CMG model with a slotted magnetic ring is proposed, which can increase output torque and reduce loss. The second part will introduce the topology and principle of the CMG. In the third part, the feasibility of the model is analyzed by finite element method (FEA). Finally, we get some conclusions in the fourth part.

II. Topology And Theory

The model shown in Fig. 1 (a) includes three parts: inner rotor, outer rotor and magnetic modulation ring, which together constitute the conventional topology of CMG. There is a layer of gap between the internal rotator and the magnetic ring as well as the magnetic ring and the external rotator, which we call the inner air gap and the outer air gap, respectively. At the air gap, the magnetic field can be adjusted by the magnetic modulation ring.

The improved CMG is shown in Fig. 1(b), and the magnetic modulation ring is slotted. At the same time, the inner rotor PMs is divided into 3 small pieces; the outer rotor PMs is divided into 2 small pieces. The 60° intervals are magnetized sequentially, and the arrows in the figure indicate the magnetization direction of each small magnet.

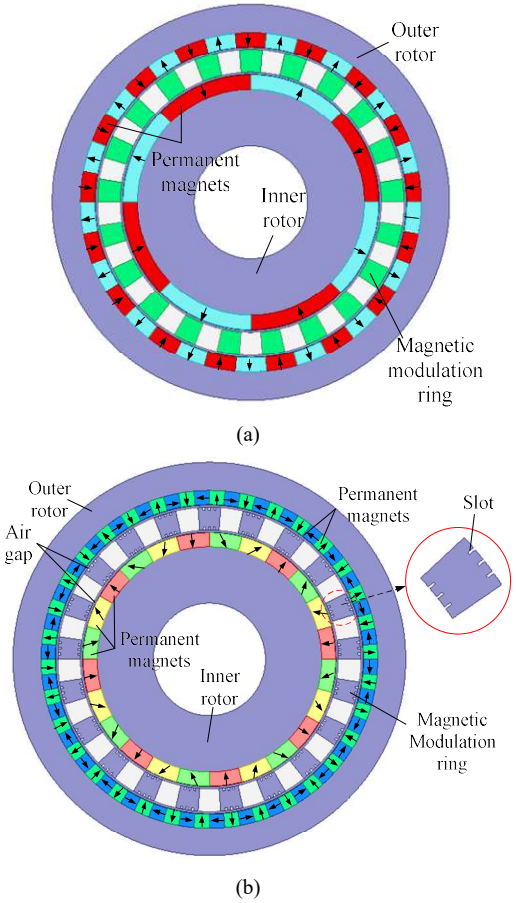

Fig. 1. CMG topology. (a) Conventional model. (b) Improved model.

The magnetic ring is used to regulate the magnetic field of the internal and external air gaps. The magnetic conductive metal and epoxy resin are alternately arranged to form the magnetic ring. In the CMG, when the flux ring is in a static state, the magnetic field of the internal and external air gap contains not only the original fundamental component, but also very rich harmonic components modulated by the flux ring. These harmonic components have corresponding spatial polar pairs and specific speed at the air gap. The spatial harmonic pole pairs of CMG air gap magnetic field can be expressed as follows

$$p_{m,k} = | mp_i + kn_s | \tag{1}$$

where m=1,3,5,7,…,∞; k =0, ±1, ±2, ±3…∞; p is the number of pole pairs of internal rotator or external rotator, n_s is the number of cores on the modulation ring. The expression between n_s and p is given by

$$n_s = p_{in} + p_{out} \tag{2}$$

where p_{in} is the number of poles of the internal rotor PMs, p_{out} is the number of poles of the external rotor PMs.

In addition, the harmonic component modulated by the flux regulating ring at the air gap also has a specific speed, which is expressed as

$$\Omega_{m,k} = \frac{mp}{mp + kn_s}\Omega_r + \frac{kn_s}{mp + kn_s}\Omega_s \tag{3}$$

where $\Omega_{m,k}$ is the angular velocity of the spatial harmonic ingredient, Ω_r and Ω_s are the rotation speed of the rotator and magnetic ring, respectively.

When k=0, the angular velocity of spatial harmonic is the angular velocity of rotor. At this time, CMG only contains inner rotor and outer rotor. When $k\neq0$, the spatial harmonic angular velocity is different from the angular velocity of the rotor. In addition to the internal and external rotors, the magnetic ring also plays a part in CMG. At this time, the angular velocity of the space harmonic components also needs to be added to the angular velocity of the magnetic rings. The stable torque transfer of the CMG must satisfy that the number of pole pairs of PMs on both rotors is equal to the number of pole pairs of spatial harmonic components. When m=1 and k=-1, the harmonic component has the largest spatial harmonic ingredient except the basic ingredient, which can be expressed as

$$\Omega_{1,-1}=\frac{p}{p-n_s}\Omega_r-\frac{n_s}{p-n_s}\Omega_s \tag{4}$$

Generally, if the magnetic ring is stationary, the transmission ratio (Gr) of the CMG can be expressed as

TABLE I
PARAMETERS OF IMPROVED CMG

Quantity	Value
Inner radius of the inner rotor yoke	20mm
Outer radius of the inner rotor yoke	40mm
Thickness of PMs on the rotor	5mm
The length of inner air gap	1mm
Thickness of stationary ring	8mm
The length of outer air gap	1mm
Inner radius of the outer rotor yoke	60mm
Outer radius of the outer rotor yoke	70mm
Axial length	60mm
Remanence of PMs	1.2T
Slotting width	0.4°
Single side slotting depth	1mm
Pole-pairs internal rotor	4
Pole-pairs external rotor	17

$$G_r=\frac{p_{out}}{p_{in}} \tag{5}$$

The torque generated by the rotor can be calculated by Maxwell Stress tensor, and its expression is

$$T_m=\frac{L_{ef}R_e^2}{\mu_0}\int_0^{2\pi}B_rB_t d\theta \tag{6}$$

where R_e is a circle of radius in the air-gap, B_r and B_t are the radial and tangential magnetic flux density, respectively. L_{ef} represents the axial length of CMG, μ_0 is the permeability of the vacuum.

III. PRFORMANCE ANALYSIS

The feasibility of the improved CMG is analyzed and verified by establishing the finite element model. Table I shows the parameters of the model.

A. Flux Density and Harmonics Analysis

The magnetic field distribution of the two models is obtained through simulation as shown in Fig. 2, and the magnetic field distribution of the improved model is shown in Fig. 2 (b). Slotting on the magnetic ring has no effect on the trend of the magnetic field lines and reduces the amount of silicon steel used; at the same times, the volume and mass of the magnetic gear are reduced.

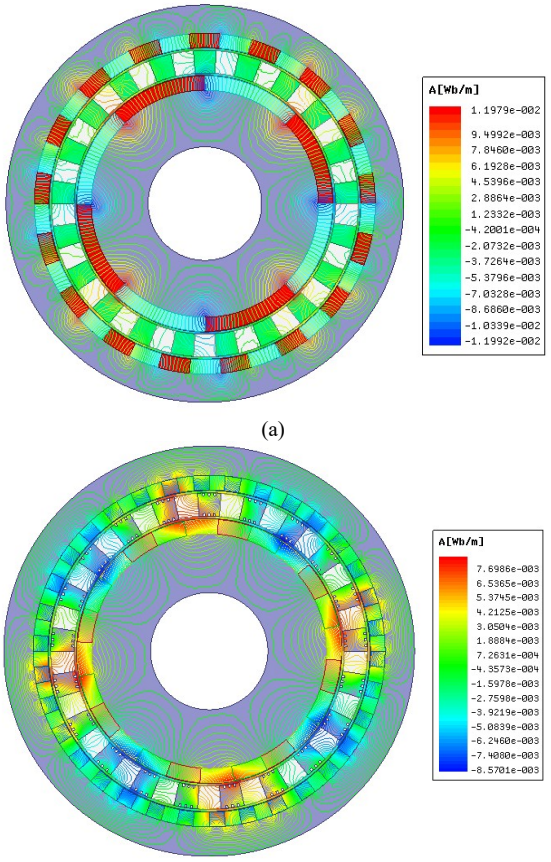

Fig. 2. Magnetic flux lines. (a) Conventional model. (b) Improved model.

At the inner air gap, the magnetic density distributions of the conventional model and the improved model in the radial and tangential directions are shown in Fig. 3. By Fourier decomposition of the magnetic density values in the radial and tangential directions, the spectrum shown in Fig. 4 is obtained. On the spectrum, we can clearly see the increase or decrease of the harmonic components.

As shown in Fig. 4, the improved CMG model significantly suppresses high-order harmonics such as 12, 20, 33, 36, 41 and 44 in radial and tangential directions.

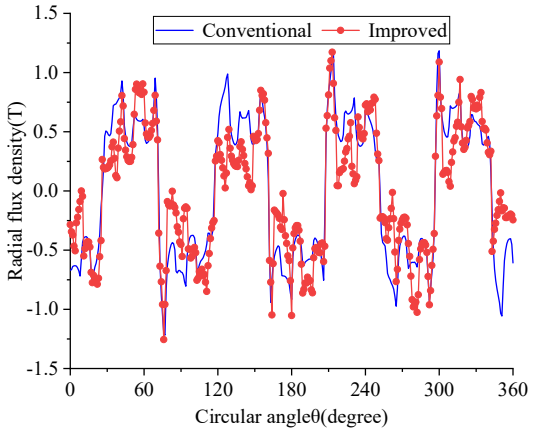

(a)

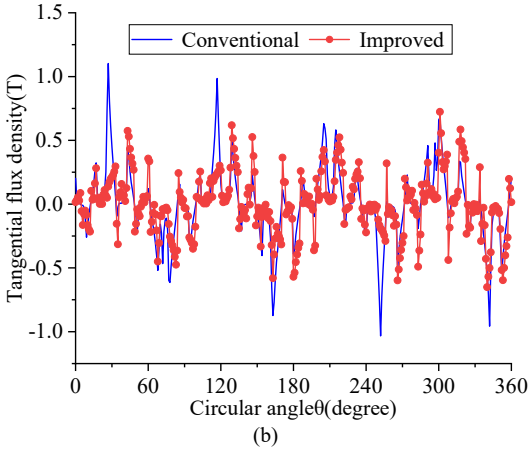

Fig. 3. Flux density distribution in the inner air gap. (a) Radial component. (b) Tangential component.

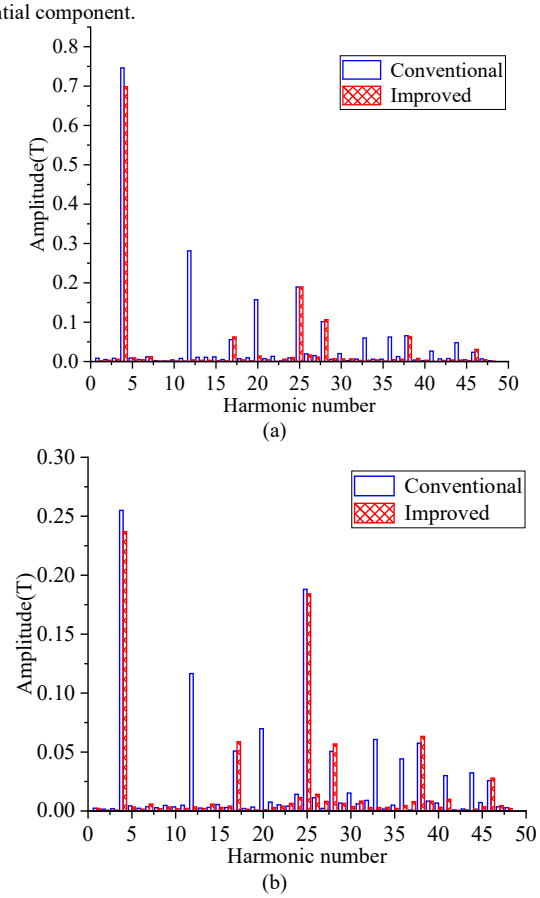

Fig. 4. Harmonic spectra of flux density in the inner air gap.(a) Radial component. (b) Tangential component.

The magnetic flux density waveform at the outer air gap is exhibit in Fig. 5, which includes radial direction and tangential direction. Whether it is the conventional structure or the improved structure, there are 17 wave heads in the radial and tangential directions, and they all have the same number of pole pairs as the PMs of the external rotor. Their flux density decomposition harmonic spectrum is shown in Fig. 6.

Fig. 6 shows the waveform after decomposing the magnetic density of the external air gap. It can be seen from the figure that the 4th, 17th, 25th and 38th harmonics have changed. Among them, the 17th harmonic is the basic harmonic of the outer air gap, and its amplitude is the largest. The increase of harmonic amplitude can change the transmission capacity of

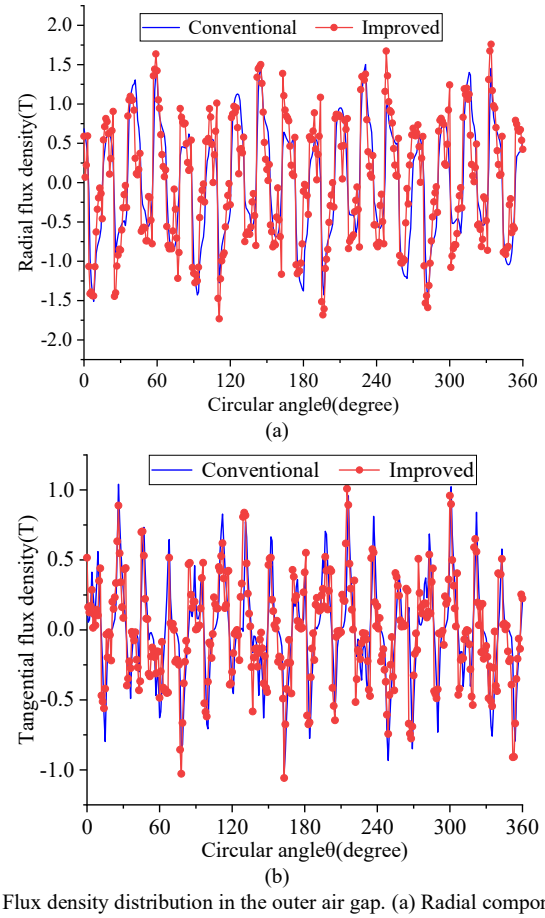

Fig. 5. Flux density distribution in the outer air gap. (a) Radial component. (b) Tangential component.

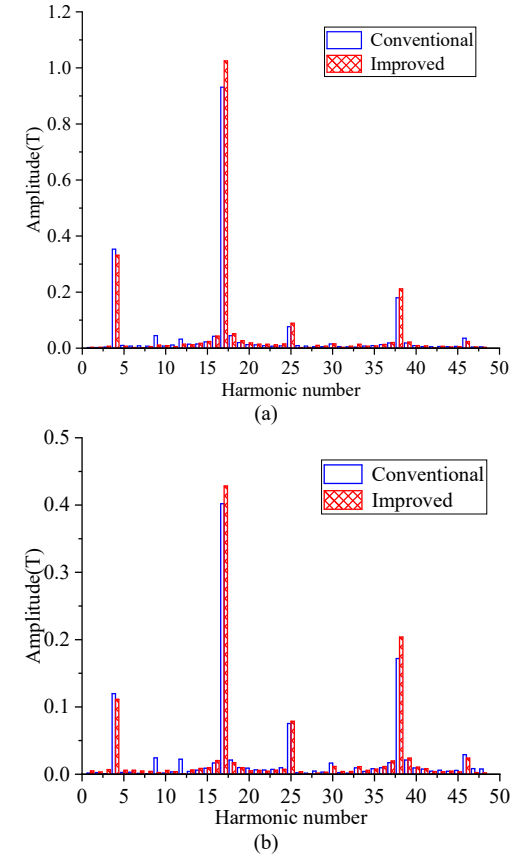

Fig. 6. Harmonic spectra of flux density in the outer air gap.(a) Radial component. (b) Tangential component.

output torque, and the amplitude of 17th harmonic of the improved model is increased, which is beneficial to the increase of transmission torque of external rotor. As for the amplitude of operating harmonic, the improved CMG is larger than the conventional model, which is helpful to improve the output torque.

B. Torque

Static torque is used to measure the load capacity of CMG. Fig. 7 shows the variation curve of CMG static torque. Fig. 7 shows the static torque fluctuation curve of the CMG.

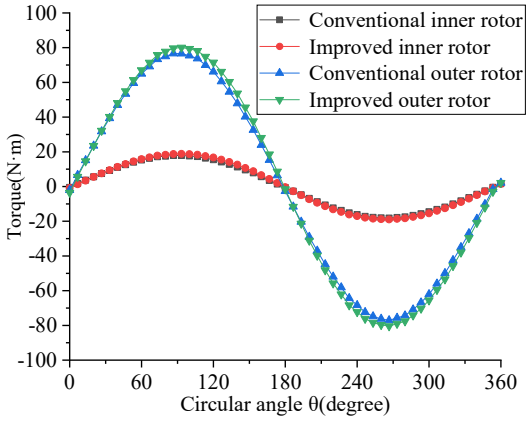

Fig. 7. Torque-angle curve.

As shown in the figure, the static torque changes in a sinusoidal curve. With the change of the curve, when the rotation angle is 93°, the curve has a peak value; at the same time, the torque ratio of inner and outer rotors is equal to the ratio of pole pairs of PMs 1:4.25.

Fig. 8 shows the comparison between the conventional model and the improved model steady-state torque. At this time, the magnetic modulation ring is in a static state, and the inner and outer rotors rotate in opposite directions at speeds of 170r/min and 40r/min, respectively. The internal torque of the conventional model and the improved model fluctuates between 17.91N·m and 18.43N·m and 18.90N·m to 19.05N·m, respectively. And the external torque of the two models fluctuate between 76.95N·m to 77.44N·m and 80.51N·m to 80.67N·m, respectively. The internal torque and external torque of the improved model are significantly higher than those of the conventional model.

The stability of torque is expressed by torque ripple, a is defined as the torque ripple coefficient, it can be expressed as follows

$$a = \frac{T_{\max} - T_{\min}}{T_{ave}} \tag{7}$$

where T_{max} is the maximum value of output torque, T_{min} is the minimum value of output torque, T_{ave} is the average value of output torque.

Table II shows the torque comparison between improved and conventional CMG. The torque of the improved CMG model is obviously greater than that of the conventional model, the average output torque of inner and outer rotors is increased by 4% and 4.12%, respectively. At the same time, the torque ripple is significantly reduced. So, the stability of the output torque is improved.

C. Loss analysis

For the eddy current loss W_{ec} generated by the PMs, it can be calculated by adding up the harmonic eddy current density loss in each harmonic, which can be expressed as

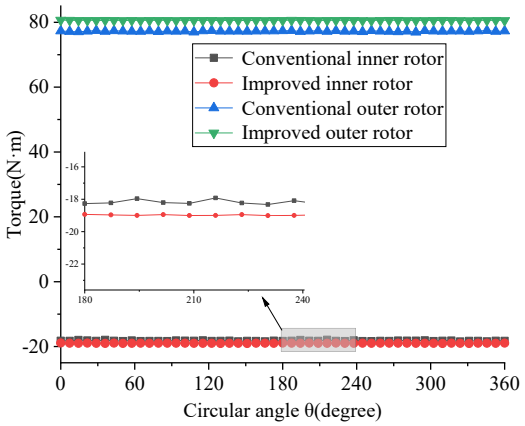

Fig. 8. Electromagnetic torque.

TABLE II
TORQUE COMPARISON OF CMG

	Types	T_{max} /(N·m)	T_{min} /(N·m)	T_{ave} /(N·m)	a%
Inner torque	I	18.43	17.91	18.21	2.85
	II	19.05	18.90	18.97	0.79
Outer torque	I	77.44	76.95	77.25	0.63
	II	80.67	80.51	80.57	0.19

$$W_{ec} = \sum_n \left(\int \frac{|J_n|^2}{2\sigma} dv\right) \tag{8}$$

where J_n is the amplitude of the nth time-harmonic, σ is the conductivity of the PMs and v is the volume of the PMs.

The loss of the inner and outer rotor yokes and the magnetic modulation ring under different harmonics can be calculated, it can be expressed as follows

$$\begin{aligned} W_{iron} &= W_{hy} + W_{ec} \\ &= \sum_n \{ \int_{iron} [A_h kf (B_{nr}^2 + B_{nt}^2) + A_e (kf)^2 (B_{nr}^2 + B_{nt}^2)] dV \} \end{aligned} \tag{9}$$

where W_{hy} is the hysteresis loss of the silicon steel sheet, W_{ec} is the eddy loss generated by the silicon steel sheet, f is the change frequency of magnetic field strength, B_{nr}, B_{nt} are the components of magnetic field intensity in radial and tangential directions, respectively. A_h and A_e are the hysteresis loss coefficient and eddy current loss coefficient of the silicon steel sheet, respectively.

Fig. 9 shows the comparison of iron consumption under different slotting depths and widths. It can be seen from the figure that when the slotting depth is certain, the volume of silicon steel on the magnetic modulation ring will decrease with the increase of slotting width, resulting in more magnetic leakage, the number of useless harmonics will increase, and the curve will show an upward trend. However, the increase of slotting width will rapidly reduce the volume of silicon steel, so the curve will decline; When the slotting degree is certain, the iron loss increases with the increase of the slotting depth. With the increase of slotting depth, the silicon steel on the magnetic

adjusting ring will be divided into blocks, which will affect the modulation of harmonics by the magnetic regulating ring and increase the amplitude of useless harmonics. When the degree and depth of slotting are both increased, the volume of silicon steel will be reduced rapidly, and the loss will be reduced. Considering the influence on the output torque while reducing the loss, the slotting width and depth are 0.4° and 1mm, respectively.

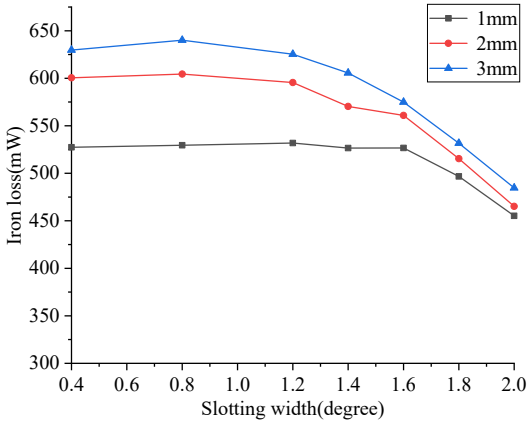

Fig. 9. Iron losses at different slotting depths and widths.

Fig. 10 shows the loss comparison between the modified and conventional CMG. In Fig. 10, the iron losses and eddy current losses of the improved CMG are smaller than those of the conventional CMG. The maximum iron loss and eddy current loss of the conventional CMG are 579.01mW and 340.69mW, respectively. The maximum iron loss and eddy current loss of the improved CMG are 527.41mW and 113.89mW, respectively. Compared with the conventional magnetic gear, the iron loss and eddy current loss are reduced by 8.9% and 66.57%, respectively.

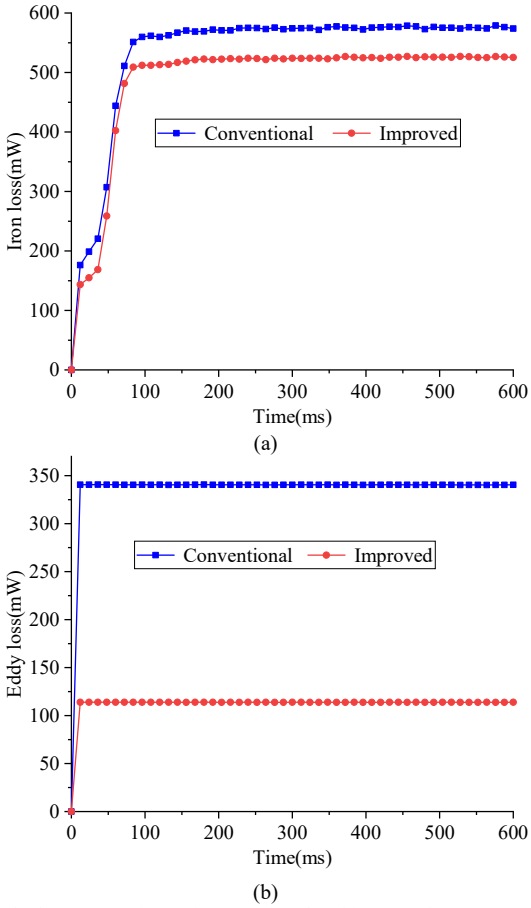

Fig. 10. The loss comparison of conventional and improved CMG. (a) Iron loss. (b) Eddy loss.

Compared with the conventional CMG model, the eddy current loss and iron loss of the proposed CMG model are reduced in varying degrees. On the one hand, the amount of silicon steel after slotting is significantly less than that of the non slotted model, so the iron consumption is reduced; On the other hand, because the Halbach array blocks the PMs, the conductivity of the whole PMs is reduced, thus reducing the eddy current loss.

D. Loss and speed

The eddy current loss and iron loss of magnetic gear are related to the permanent magnet on the two rotors, the yoke on the two rotors and the flux adjusting ring, respectively. The FEA is used to analyze the loss. According to the transmission ratio of 4.25:1, the speed of the inner rotor is gradually increased from 100r/min to 1700r/min. The relationship curves between iron loss, eddy current loss and speed are obtained, as shown in Fig. 11.

It can be seen from Fig. 11 that in a given speed range, the iron loss and eddy current loss of CMG increase with the acceleration of inner rotor speed, and the increase of loss will cause the decrease of efficiency. When the inner rotor speed is 200r/min, the iron loss is 196.3mW and the eddy current loss is 178mW. When the inner rotor speed is 300r/min, the iron loss is 353.6mW and the eddy current loss is 398.7mW. With the increase of rotating speed, the loss also increases. Therefore, while increasing the torque, we should also control the rotating speed of the CMG to achieve the effect of large torque and low loss.

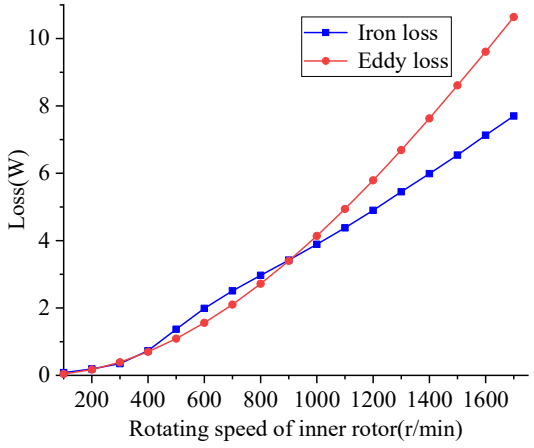

Fig. 11. Variation curve of loss and speed.

IV. Conclusion

In this paper, a CMG with slotted magnetic modulation ring is proposed and analyzed. The internal and external rotors PMs are equally divided and Halbach array is adopted. At the same time, the slotted width and depth of the magnetic ring are 0.4° and 1mm, respectively. The improved CMG is analyzed and

calculated by FEA. The results show that the static torque of the proposed model is amplified, and the torque ratio of the internal and external rotors meets the ratio of the number of pole pairs of PMs of 1:4.25. In addition, the average torque of the two rotors is 4% and 4.12% higher than that of the conventional CMG, respectively; the ripple was reduced by 72.28% and 69.84%, respectively. And the iron loss and eddy current loss are reduced by 8.91% and 66.57%, respectively compared with the conventional model. Finally, the curve of loss with speed is given, it is concluded that in order to ensure the operating efficiency of CMG, We should control its speed.

REFERENCES

[1] J. Q. Liu, J. G. Bai, G. P. Liu, Y. T. Wang and P. Zheng, "Investigation of an integrated magnetic-field-modulated brushless double-rotor machine with an improved PM rotor," *IEEE Trans. Magn.*, vol. 57, no. 2, pp. 1-6, Feb. 2021.

[2] X. Ren, D. W.Li, R. H. Qu and T. H. Pei, "Back EMF harmonic analysis of permanent magnet magnetic geared machine," *IEEE Trans. Ind. Electron*., vol. 67, no. 8, pp. 6248-6258, Aug. 2020.

[3] M. C. Gardner, M. Johnson and H. A. Toliyat, "Comparison of surface permanent magnet axial and radial flux coaxial magnetic gears," I*EEE Trans. Energy Convers.*, vol. 33, no. 4, pp. 2250-2259, Dec. 2018.

[4] K. Jenney and S. Pakdelian, "Magnetic design aspects of the trans-rotary magnetic gear using Quasi-Halbach arrays," *IEEE Trans. Ind. Electron*., vol. 67, no. 11, pp. 9582-9592, Nov. 2020.

[5] L. B. Jing, T. Zhang, Y. T. Gao, R. H. Qu, Y. H. Huang and T. Ben, "A novel HTS modulated coaxial magnetic gear with eccentric structure and Halbach arrays," *IEEE Trans. Appl. Supercond.*, vol. 29, no. 5, pp. 1-5, Aug. 2019.

[6] L. B. Jing, Y. L. Pan, T. Wang, R. H. Qu and P. T. Cheng, "Transient analysis and verification of a magnetic gear integrated permanent magnet brushless machine with Halbach arrays," *IEEE Journal of Emerging and Selected Topics in Power Electronics*, vol. 10, no. 2, pp. 1881-1890, Apr. 2022.

[7] M. Johnson, M. C. Gardner, H. A. Toliyat, S. Englebretson, W. Ouyang and C. Tschida, "Design, construction, and analysis of a large scale inner stator radial flux magnetically geared generator for wave energy conversion," *IEEE Energy Conversion Congress and Exposition (ECCE),* 2017, pp. 5017-5024.

[8] L. B. Jing, Z. X. Huang, J. L. Chen and R. H. Qu, "Design, analysis, and realization of a hybrid-excited magnetic gear during overload," *IEEE Trans. Ind. Appl.*, vol. 56, no. 5, pp. 4812-4819, Sept.-Oct. 2020.

[9] K. Aiso, K. Akatsu and Y. Aoyama, "Motor system integrated magnetic multiple spur gear and high speed motors for electric vehicle," *2020 IEEE Energy Conversion Congress and Exposition (ECCE)*, 2020, pp. 68-74.

[10] H. Y. Wong, J. Z. Bird, D. Barnett and W. Williams, "A high torque density Halbach rotor coaxial magnetic gear," *2019 IEEE International Electric Machines & Drives Conference. (IEMDC)*, 2019, pp. 233-239.

[11] L. N. Jian, Z. X. Deng, Y. J. Shi, J. Wei and C. C. Chan, "The mechanism how coaxial magnetic gear transmits magnetic torques between its two rotors: detailed analysis of torque distribution on modulating ring," *IEEE/ASME Trans. Mechatronics*, vol. 24, no. 2, pp. 763-773, 2019.

[12] L. B. Jing, J. Gong, Z. X. Huang, T. Ben and Y. H. Huang, "A new structure for the magnetic gear," *IEEE Access*, vol. 7, pp. 75550-75555, 2019.

[13] H. Zhao, C. H. Liu, Z. X. Song and J. C. Yu, "A fast optimization scheme of coaxial magnetic gears based on exact analytical model considering magnetic saturation," *IEEE Trans. Ind. Appl.*, vol. 57, no. 1, pp. 437-447, Jan.-Feb. 2021.

[14] Y. Y. Ni, X. Jiang, B. X. Xiao and Q. J. Wang, "Analytical modeling and optimization of dual-layer segmented Halbach permanent-magnet machines," *IEEE Trans. Magn.*, vol. 56, no. 5, pp. 1-11, May 2020.

[15] J. X. Shen, H. Y. Li, H. Hao and M. J. Jin, "A coaxial magnetic gear with consequent-pole rotors," *IEEE Trans. Energy Convers.*, vol. 32, no. 1, pp. 267-275, March 2017.

[16] L. B. Jing, L. Liu, M. Xiong and D. Feng, "Parameters analysis and optimization design for a concentric magnetic gear based on sinusoidal magnetizations," *IEEE Transactions on Appl. Supercond.*, vol. 24, no. 5, pp. 1-5, Oct. 2014.

[17] S. J. Kim, E. Park, S. Jung and Y. Kim, "Transfer torque performance comparison in coaxial magnetic gears with different flux-modulator shapes," *IEEE Trans. Magn.*, vol. 53, no. 6, pp. 1-4, June 2017.

[18] X. X. Zhang, X. Liu and Z. Chen, "A novel dual-flux-modulator coaxial magnetic gear for high torque capability," *IEEE Trans. Energy Convers.*, vol. 33, no. 2, pp. 682-691, June 2018.

[19] Z. Xiang, X. Zhu, M. Jiang and L. Quan, "Multi-objective-layered optimization of a magnetic planetary gear for hybrid powertrain," *IEEE Journal of Emerging and Selected Topics in Power Electron*., vol. 10, no. 1, pp. 934-944, Feb. 2022.

[20] M. C. Gardner, B. E. Jack, M. Johnson and H. A. Toliyat, "Comparison of surface mounted permanent magnet coaxial radial flux magnetic gears independently optimized for volume, cost, and mass," *IEEE Trans. Ind. Appl.*, vol. 54, no. 3, pp. 2237-2245, May-June 2018.

[21] M. Johnson, M. C. Gardner and H. A. Toliyat, "Design comparison of NdFeB and ferrite radial flux surface permanent magnet coaxial magnetic gears," *IEEE Trans. Ind.Appl.*, vol. 54, no. 2, pp. 1254-1263, March-April 2018.

[22] T Fujita, Y Ando, and K Nagaya, "Surface magnet gears with a new magnet arrangement and optimal shape of stationary pole pieces," *Journal of Electromagnetic Analysis & Applications*, vol.5, no.6, pp. 243-249, 2013.

[23] R. Zanis, A. Borisavljevic, J. W. Jansen and E. A. Lomonova, "Iron loss investigation of miniaturized magnetic gears having solid cores," *2014 17th International Conference on Electrical Machines and Systems (ICEMS)*, 2014, pp. 3078-3082.

[24] S. Gerber and R-J. Wang, "Evaluation of a prototype magnetic gear," *2013 IEEE International Conference on Industrial Technology (ICIT)*, 2013, pp. 319-324.

Can Tan was born in Chongqing, China. He received his B.S degree in electrical engineering from Langfang Teachers College in 2020. He is currently working towards the M.S. in China Three Gorges University. His research interest includes electromagnetic field analysis design of magnetic gear and motor.

Wei Liu received B.S degree in electrical engineering from Henan University of Engineering in 2020. He is currently working towards the M.S. in China Three Gorges University. His research interest includes electromagnetic field analysis design of magnetic gear and motor.

Yingying Rao received B.S degree in electrical engineering and automation from the North China Electric Power University Science Technology College in 2019. She is currently working towards the M.S. in China Three Gorges University. Her research interest includes switch reluctance motor.

Weizhao Tang received B.S degree in electrical engineering and automation from the North China Electric Power University Science Technology College in 2020. He is currently working towards the M.S. in China Three Gorges University. His research interest includes electromagnetic field analysis design of multi air gap magnetic field motor.

Libing Jing was born in Henan province, China. He received his B.S degree from Zhongyuan University of Technology in 2006 and the Ph.D. degree from Shanghai University in 2013. Since July 2016, He has been an associate professor in the College of Electrical Engineering and New Energy, China Three Gorges University. Dr. Jing has authored over 90 published technical papers and is the holder of over 10 patents/patent applications. He was recipient of the Best Poster Presentation Award from the 4th International Conference on Intelligent Green Building and Smart Grid (IGBSG 2019).

His research activities are related to design, modeling, and analysis of electrical machines.